Best practice strategies for validation of micro moulding process simulation

F.S. Costa[(1)], G. Tosello[(2)], B.R. Whiteside[(3)]

(1) Autodesk Inc, MFG-Digital Factory, 259-261 Colchester Road Kilsyth, Australia

(2) Technical University of Denmark (DTU), Department of Mechanical Engineering, Building 427S, DK-2800 Kgs. Lyngby, Denmark

(3) IRC in Polymer Science and Technology, School of Engineering, Design and Technology, University of Bradford, Bradford BD7 IDP UK

Abstract

Simulation programs in polymer micro replication technology are used for the same reasons as in conventional injection moulding. To avoid the risks of costly re-engineering, the moulding process is simulated before starting the actual manufacturing process. Important economic factors are the optimization of the moulding process and of the tool using simulation techniques. Therefore, in polymer micro manufacturing technology, software simulation tools adapted from conventional injection moulding can provide useful assistance for the optimization of moulding tools, mould inserts, micro component designs, and process parameters. In order to obtain reliable results, adapted simulations to micro moulding applications need to be validated by comparison with experimental results. Due to the miniaturized scale of the part and the extreme conditions of the process, accurate process monitoring is challenging and therefore software

validation is affected by the availability of adequately precise experimental data. In this paper, an investigation on two different micro moulded parts is presented and issues relating to the use of experimental results for the validation of micro moulding simulations are discussed. Recommendations regarding sampling rate, meshing quality, filling analysis methods (micro short shots, flow visualization) and machine geometry modelling are given on the basis of the comparison between simulated and experimental results within the two considered study cases.

1. Introduction

The use of simulation for injection moulding design is a powerful tool which can be used up-front to avoid costly tooling modifications and reduce the number of mould trials. However, the accuracy of the simulation results depends on many component technologies and information, some of which can be easily controlled or known by the simulation analyst and others which are not easily known. For this reason, experimental validation studies are an important tool for establishing best practice methodologies for use during analysis set up on all future design projects. During the validation studies, detailed information about the moulding process is gathered and used to establish these methodologies. Whereas in routine design projects, these methodologies are then relied on to provide efficient but reliable working practices.

Validation studies in the area of micro-injection moulding are complicated by three additional factors:

A. the difficulty of sensor placement within the reduced dimensions of the mould and moulding cavity,
B. the speed of the moulding process, and
C. the potential for altered physics due to the smaller part feature and moulding machine size.

Placement of sensors such as pressure sensors will often not be possible in the reduced dimensions of the moulding cavity and so alternative locations for the sensors must be employed. For example, the pressure transducers may be located in the feed system, where larger dimensions than the cavity exist, but this means that direct validation of cavity pressure values predicted by simulation is not possible.

Timing of data acquisition and the accuracy of these recordings become important in the high injection speeds used for micro moulding.

Numerous approximations traditionally made for conventional injection moulding simulation may become invalid for micro moulding. One example of this is the heat transfer coefficient used to model the heat flux across the interface of the polymer and mould metal. Values typically used in conventional injection moulding are derived from experiments performed on typical cavity thicknesses above 1mm [1]. These heat transfer coefficient values may not be appropriate in a simulation of the packing phase of micro-injection moulding; usually a constant heat transfer coefficient (HTC) is assumed, but it cannot describe the flow

through micro channels and its standard value suitable for simulation of macro parts differs substantially from values indicated for μIM [2] [3] [4]. Moreover, one of the main limitations encountered in micro moulding simulations relates to the fact that rheological data used in current packages are obtained from macroscopic experiments and that a no-slip boundary condition is employed with the consequence that wall slip cannot be predicted [2]. On the other hand, standardized micro capillary rheology testing equipments and procedures are currently not available. Additionally, even though experimental investigation has shown the presence of wall slip on polymer melt flow in micro scaled channels and its influence on viscosity [5], rheological models suitable for software implementation are far from being formulated. Moreover, surface tension, neglected in macro moulding, plays a role on the filling of micro structures but is not taken into account [6].

Another approximation typically used is that part width and length are much larger than the part thickness, and so shell based solutions techniques can be used. These shell based solutions employ the Hele-Shaw assumptions to simplify the computation domain and reduce the time and cost of computation. According to the Hele-Shaw assumptions, the pressure is assumed to be uniform through the part thickness, the flow resistance due to drag on the cavity edges is neglected, thermal convection is neglected in the thickness direction and thermal conduction is neglected in all directions except for the thickness direction [7] [8]. However, such Hele-Shaw assumptions are not valid for micro moulding parts which

more typically have length and width scales similar to their thickness scales. Therefore, the use of true three-dimensional simulation models is preferred.

2. Experiments

Two sets of micro moulding experiments are used in this work. These are the moulding of a dog-bone shaped tensile bar sample and of a thin flat cavity with an obstacle.

2.1 Dog-bone shaped tensile bar sample:

These parts were moulded on a FormicaPlast 1k (i.e. one-component) micro moulding machine from DESMAtec which is provided by a two-plunger plastication/injection unit (see Figure 1).

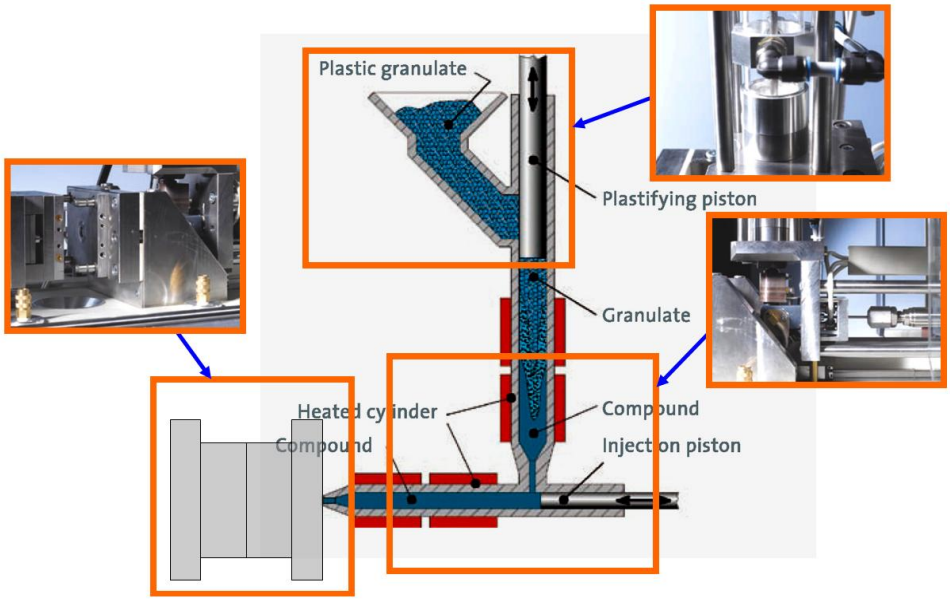

Figure 1 Two stage (plastication and injection) unit and micro mould of the employed micro injection moulding machine [9]

The mould was a two cavity mould as shown in Figure 2, with an approximate part thickness of 1 mm, width ranging from 1.5 mm to 3 mm

and a part length of 12 mm. The whole molding including the miniaturized sprue, two runners and two parts had a weight of 93.8mg (with a standard deviation of 0.2mg on a sample of 10 parts randomly selected over 50 parts). The moulding experiments were performed using a BASF Ultraform H2320 004 POM material.

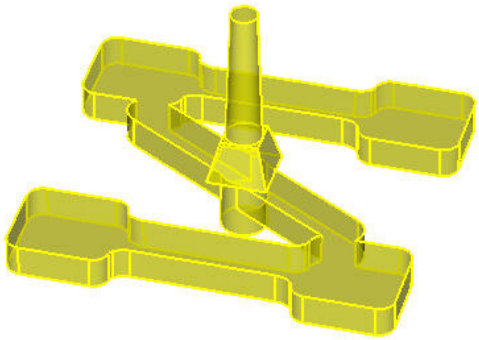

Figure 2 Two-cavity dog-bone tensile bar moulding

The moulding procedure was conducted as a continuous process with part ejection operated by miniaturized mechanical pins. Moulding of production batches included first a temperature stabilization time of about 10 minutes, then a moulding series of about 25 parts followed by an actual series of 50 parts suitable for process and part analysis. Process data was automatically collected by in-built sensors in the machine for each moulding cycle and included: shot stroke, injection speed, injection pressure, mould temperature in both sides of the mould and melt temperature in four different locations of the injection unit (injection nozzle, end of dosing chamber, middle and beginning injection chamber). Set mould and melt temperatures were 50°C and 220°C respectively and standard deviation over the whole production batch was of 0.1°C for both temperatures. Figure 3 shows the average and standard deviation of the

pressure and velocity profiles recorded during the filling stage of 20 parts. Injection was completed in 0.1 seconds. Standard deviation for velocity and stroke length is very low throughout the entire process. The piston accelerated for a stroke length of 3mm prior to the actual start of the melt injection in order to be able to provide the requested speed at the beginning of the full length stroke. The machine capability is limited in this phase: a maximum acceleration of 6mm/s^2 can be provided by the piston.

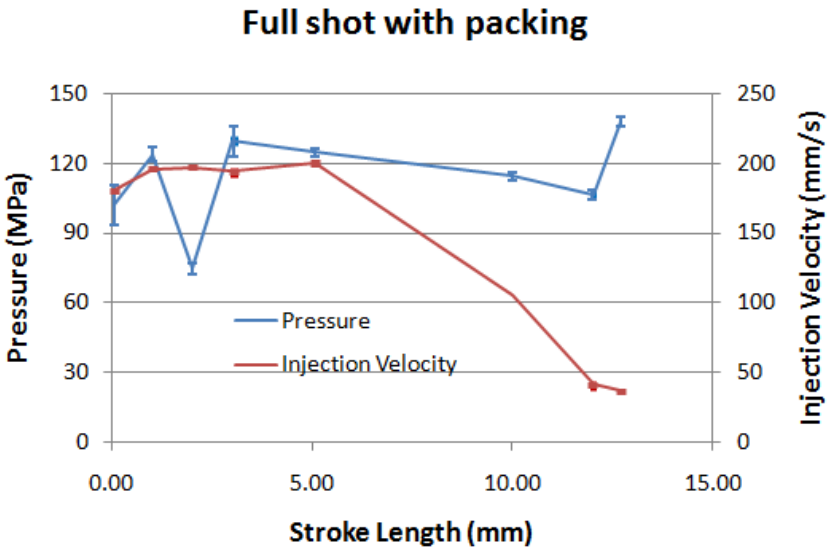

Figure 3 Speed and injection pressure profile during filling and packing phases of the two-cavity dog-bone shaped tensile bar sample

The piston followed the set speed profile for a stroke length of 12.70mm until the point of switchover to the packing phase. However, this stroke length gives a stroke volume of 89.77 mm^3, which is greater than the mould volume to be filled of 75 mm^3. If the full stroke from 23 mm to 10.3 mm is used for the velocity control phase of injection, the cavity should fill before the point of switch-over to pressure control is reached. The reason for this stroke volume excess is believed to be the backflow of polymer from the injection chamber back into the metering chamber which

occurs during injection until the injection chamber is sealed off from the metering chamber when the injection piston reaches the 21 mm position. The 21 mm position is assumed based on required volume required to fill the cavity. Actual internal dimensions of the machine are not known.

Intermediate filling stages and product repeatability were investigated by means of measuring part weight and length for a series of short shots moulding trials. Process resolution and robustness was proven to be a function of the stroke length, increasing towards complete filling (see Table 1). This demonstrates the difficulty to produce highly repeatable parts when moulding short shots with weight of tens of milligrams at high injection speed and thus the difficulty to actually use these results for micro moulding simulation validation.

Table 1 Short shots characterization at different stroke lengths

Stroke length	5mm	7mm	8mm	9mm	11mm	12.7mm (part completely filled)
Short shots						
Average Weight	58.3mg	66.1mg	69.8mg	73.8mg	82.9mg	93.8mg
Std dev. Weight	2.6mg	2.0mg	1.4mg	1.8mg	1.5mg	0.2mg
Average Part length	5.88mm	7.91mm	8.52mm	9.62mm	10.86mm	11.67mm
Std. dev Part length	0.48mm	0.11mm	0.15mm	0.15mm	0.13mm	0.01mm

2.2 Thin flat cavity

A flat cavity of thickness 0.25 mm, width 3.5 mm and length 7.5 mm as shown in Figure 4 was moulded on a Battenfeld Microsystem 50 machine. Although this cavity geometry might be suitable for a Hele-Shaw shell based simulation, there are aspects of the runner system feeding this cavity which are not well suited to a Hele-Shaw analysis and so only a 3D simulation of this geometry will be considered in this study. An additional reason for focusing on the 3D simulation of this geometry is that these validation studies aim to establish the best practices for simulation methodologies for general micro injection moulding parts and such parts are typically more complex and are not well suited to Hele-Shaw shell based analysis.

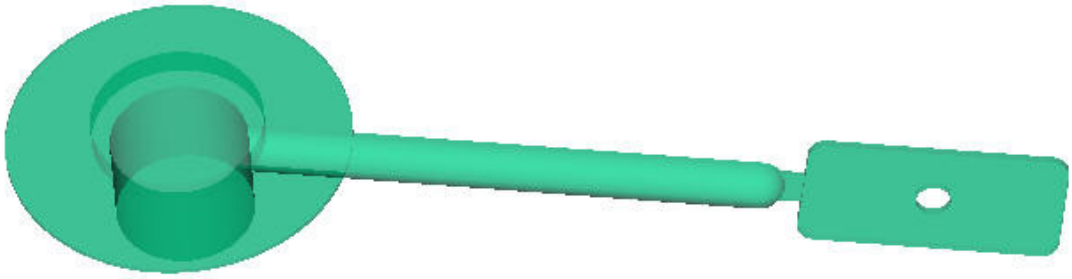

Figure 4 Thin flat cavity and feed system

Injection occurs on the top face of the large flat disc region at the left of Figure 4 and the cavity is shown on the right side with a 1 mm hole in its centre.

In an initial experimental study of this mould using a BASF Polystyrene 158K, the influence of injection speed and mould temperature on the flow

front shape was examined. Three mould temperatures were used, being 50°C, 80°C and 110°C. At each mould temperature, three injection piston velocities of 25 mm/s, 50 mm/s and 100 mm/s were used. In all cases, the melt temperature was 220°C. The mould includes a transparent sapphire window on one half of the mould cavity and a high speed camera was used for image capture during the cavity filling to record the flow front position [1]. A frame rate of 740 images per second was used, however, even this frame rate was relatively too slow for the high speed filling of the cavity which occurred, meaning there was some difficulty to select images at corresponding flow front positions. Some comparisons were possible as shown in Figure 5 and 6. Images were selected as close as possible to the time at which the flow fronts rejoin after passing around the hole (obstacle) in the cavity. Although exact comparison is hampered by the low frame rate, comparison of the flow front shapes at 25 mm/s and 100 mm/s injection speeds in Figure 5 for a 50°C mould temperature reveals that injection speed has very little effect on flow front shape. Similarly, Figure 6 compares the flow front shape for 100 mm/s injection and 50°C mould temperature to the flow front shape for 50 mm/s injection and 110°C mould temperature. This comparison also shows very little variation in flow front shape, despite the large difference in mould temperatures. Therefore, visualisation of flow front shape alone is not considered to be a sufficient mechanism for validation of simulation results, however it can be a useful aid in understanding the filling sequence.

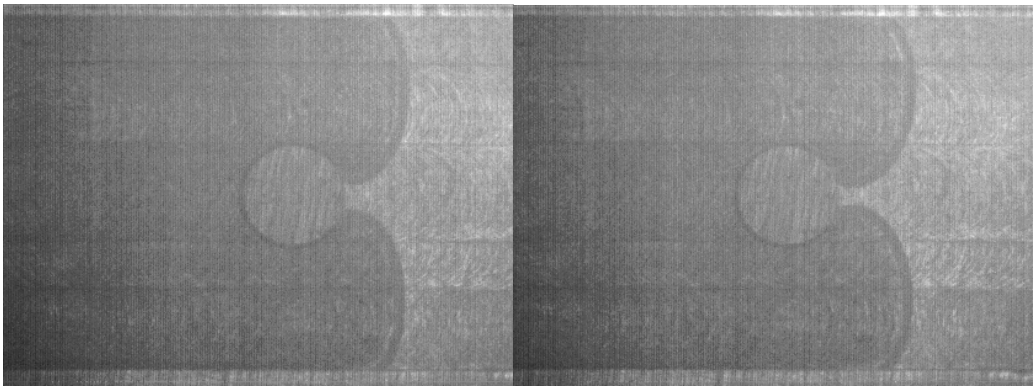

Figure 5 Comparison of flow front shapes for 25 mm/s and 100 mm/s injection at 50°C mould temperature

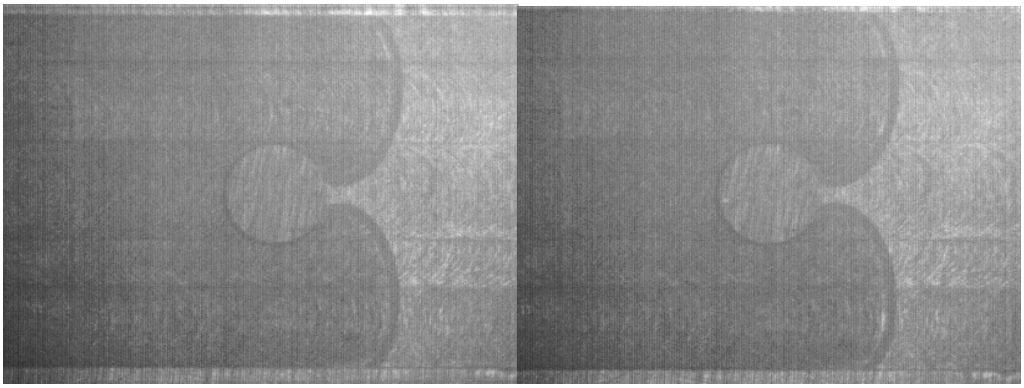

Figure 6 Comparison of flow front shapes for 100 mm/s & 50°C and 50 mm/s & 110°C

A second experimental study on this thin flat cavity was conducted where injection pressure was captured by a pressure sensor located under the ejector pin and piston velocity data was also obtained from magnetostrictive velocity/displacement transducer. The ejector pin is located underneath the flat disc injection location and the pressure sensor is a piezoelectric pressure/force transducer. In this second experimental study 3400 images per second were captured of the lower half of the cavity. In this series of experiments, mouldings with constant piston velocity of: 60 mm/s, 120 mm/s, 240 mm/s and 480 mm/s were made. The material used in this second experimental study was Ineos 100-GA12 PP.

Analysis of the injection pressure and piston velocity data reveals some interesting features, which should correspond to discrete events in the mould filling sequence. These features are illustrated in the graph for the 480 mm/s injection speed in Figure 7. This figure only shows the portion of data relevant to the period when the cavity was filling. The step nature of the flow rate data is believed to indicate that the sensor response rate was lower than the sampling rate.

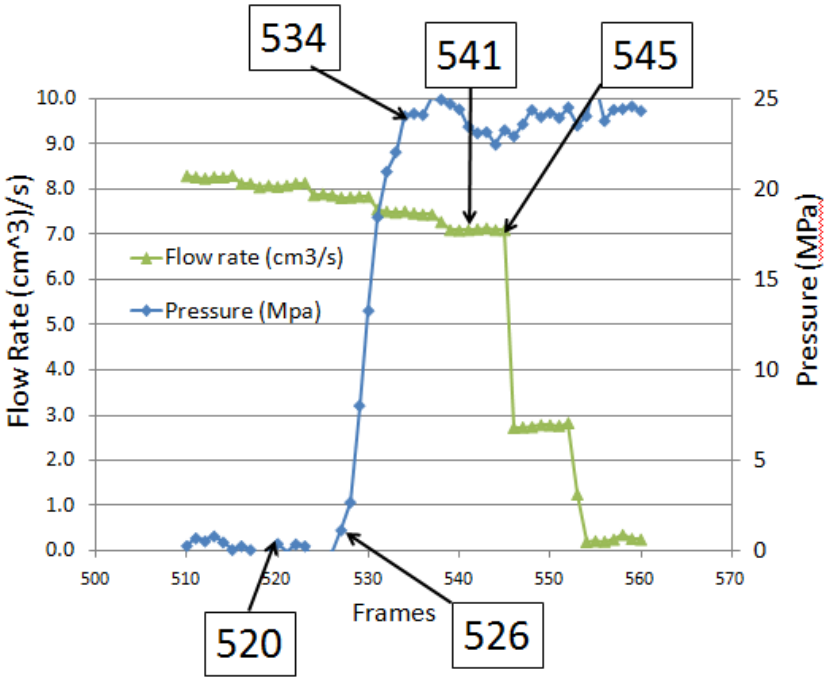

Figure 7 Injection pressure and flow rate for 480 mm/s injection speed

The apparent limiting of the injection pressure to around 25 MPa in this case is not due to any process setting. Rather, there are compressible washers used in the mounting of the injection unit. Above a critical pressure, these washers are believed to compress to protect the injection unit from rapid pressure spikes during high speed injection when the

cavity fills. Although the injection unit is still delivering injection at the programmed flow rate, backward movement of the injection unit as the washers are compressed effectively limits the injection pressure.

In Figure 7, various events in the data could be interpreted to correspond to key events in the process. For example, because the feed system is much thicker than the gate and cavity, it is reasonable to assume that injection pressure will begin to rise sharply when the flow front begins to fill the gate and cavity. This is expected to correspond to the inflection in the pressure data which occurs at frame 526. Similarly, frame 534 can be interpreted as the instant when critical pressure limit was reach. Frame 545 could correspond to the instant that the cavity is first filled, thus causing injection speed to be dramatically reduced. However, in this study, we also have the benefit of the high speed image capture of the flow front position and we can therefore test these assumed event interpretations. Figure 8 shows the flow front images captured at frames 520, 526 and 541. The flow front position in frame 520 shows that the cavity begins filling at this frame, rather than at frame 526. Frame 541 is the first image captured when the cavity filling has completed, indicating that 545 can not correspond to the end of cavity filling.

A number of possible reasons may be the cause of this lack of correlation between the captured images and the observed injection pressure and piston velocity data:

- Data filtering on pressure and velocity signals

- Inadequate sampling rate on pressure and velocity signals
- Errors in image and data timing

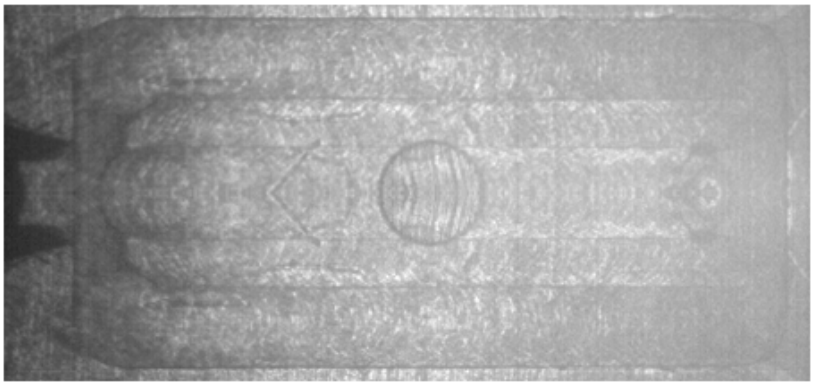

Frame 520

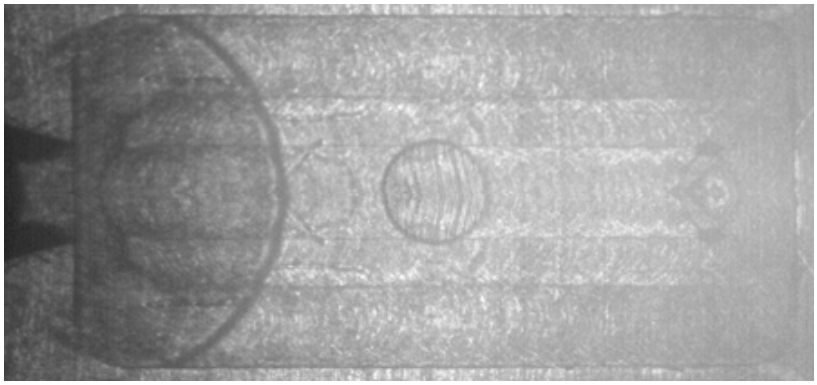

Frame 526

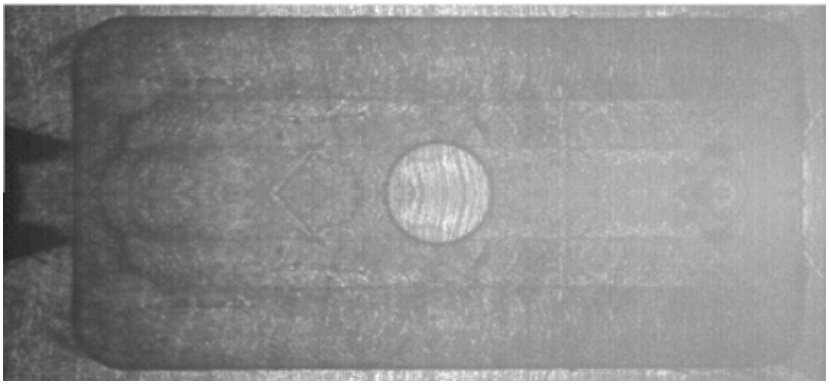

Frame 541

Figure 8 Flow front positions at frames 520, 526 and 541 during 480 mm/s injection of the thin flat cavity

The injection pressure and flow rate graphs from injection speeds of 120 mm/s and 240 mm/s have all the same features as Figure 7. However, the injection pressure data for the moulding at a speed of 60 mm/s is somewhat different. As shown in Figure 9, injection pressure rises up to a much higher pressure (around 120 MPa); however, most of this pressure rise appears to occur after the cavity has completely filled.

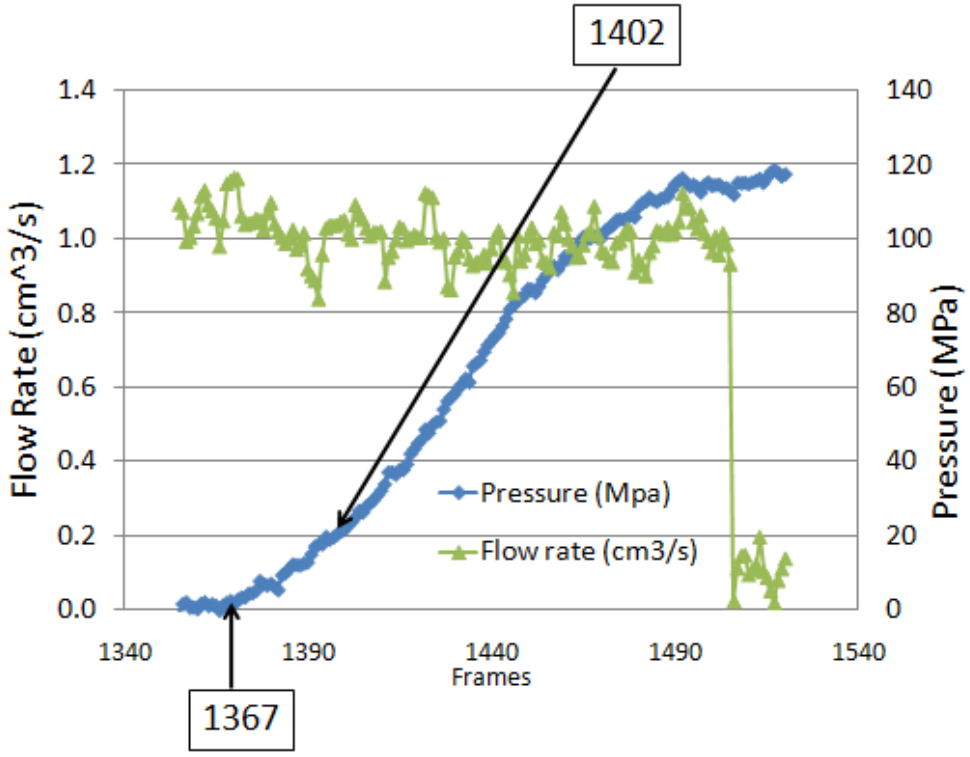

Figure 9 Injection pressure and flow rate for 60 mm/s injection speed

The instant when injection pressure begins rising in Figure 9 is frame 1367, whereas the flow front was observed to reach the gate much earlier at frame 1283. The first image of the cavity completely filled was at frame 1402, whereas injection pressure continues to rise steadily for 200 frames after this. These flow front position images are shown in Figure 10.

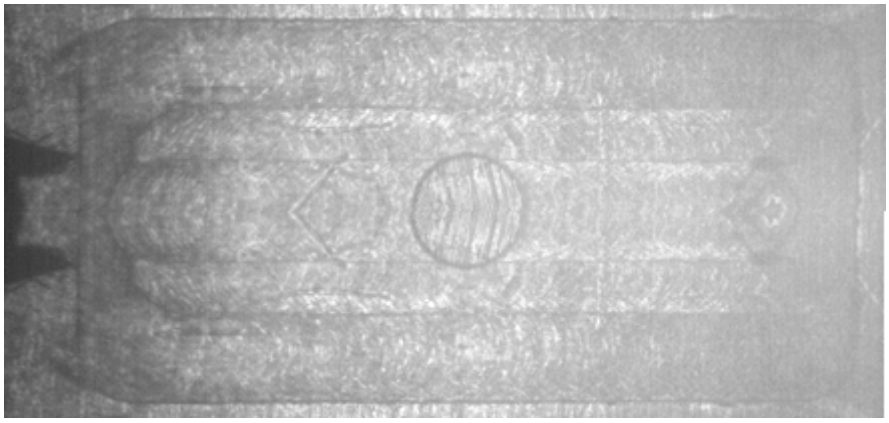

Frame 1283

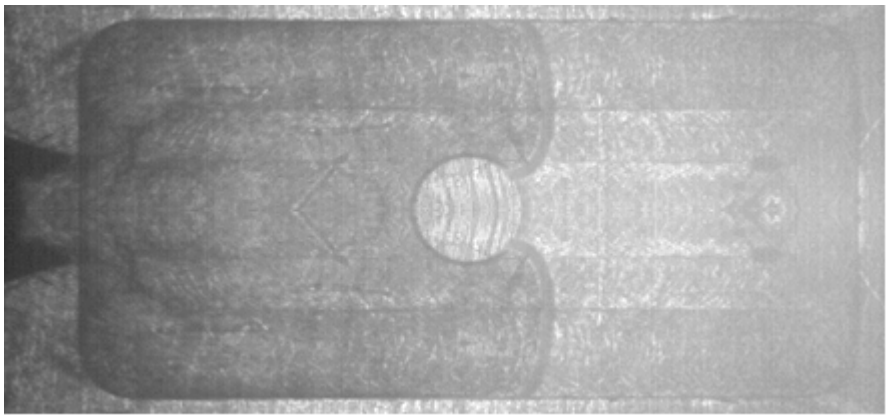

Frame 1367

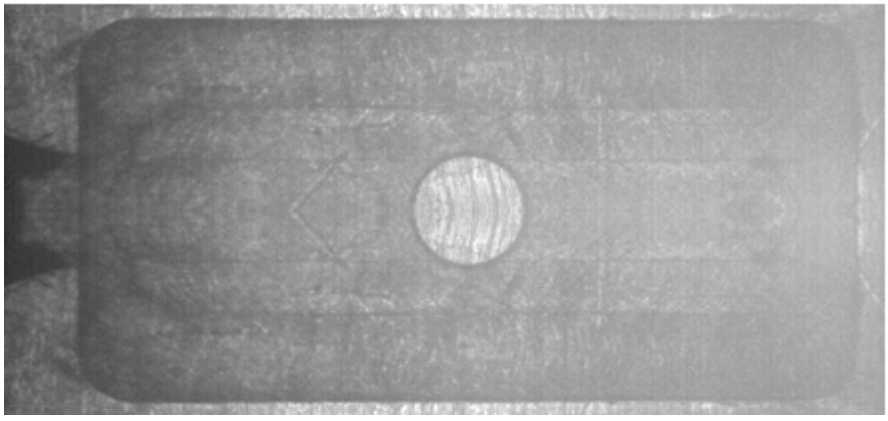

Frame 1402

Figure 10 Flow front positions at frames 1283, 1367 and 1402 during 60 mm/s injection of the thin flat cavity

In the case of this 60 mm/s moulding, the lack of correlation between the captured images and the features of the injection pressure and flow rate

data is even stronger than it was for the 480 mm/s moulding. In particular, doubts are raised about the maintaining of a near constant flow rate even long after the instant where cavity filling has completed. A possible explanation for this relates to the thin disc volume around the injection location. This disc volume is formed where the injection nozzle comes in contact with the bushing on the mould. If the compressible washers are allowing the injection unit and nozzle to move backward once a critical pressure is reached, then the thickness of the disc volume will be increasing, which allows the injection unit to continue to deliver a constant flow rate even after the cavity has filled.

From the captured images of the cavity filling and the known frame rate, it is possible to determine the time which elapsed during the cavity filling at each set flow rate. These are shown in Table 2.

Table 2: Observed cavity fill times for thin flat cavity

Set Velocity (mm/s)	Set Flow Rate (mm^3/s)	Start of cavity filling (frame #)	End of cavity filling (frame #)	Number of Frames	Time to fill cavity (sec)	Apparent Cavity Flow Rate (mm^3/s)
60	1,178	1285	1402	117	0.034	186
120	2,356	724	777	53	0.016	395
240	4,712	303	333	30	0.0088	717
480	9,425	521	541	20	0.0059	1,070

Given the cavity volume of approximately 6.31 mm^3, these cavity filling times can be converted into apparent average cavity flow rates. These

average cavity flow rates achieved are between 6 and 9 times lower than the set flow rates. This is believe to be because of the critical pressure for compression of the washers being reached during cavity filling and that polymer melt is being retained at the nozzle tip to fill the expanding disc volume under the nozzle. These cavity flow rates are averages only. From the capture flow front images, it was observed that the cavity filling rate was faster at the end that it was at the beginning of cavity filling.

3. Mesh Preparation for Simulation

Simulations were run and three-dimensional analysis meshes were prepared using the Autodesk Moldflow Insight 2010-R2 product. From three-dimensional CAD models of both geometries, a surface mesh comprising triangular elements was first created. Following this, a three-dimensional volume mesh of tetrahedral elements was created.

During the creation of the surface mesh, particular care is required specific to the micro moulding geometry. Although the Autodesk Moldflow software will choose a default mesh size based on the overall geometry, this will typically be too coarse for a micro-injection moulding cavity if the feed system is disproportionately larger than the cavity. In this current work, both geometries were meshed with a surface mesh size of 0.1 mm. In addition, the Autodesk Moldflow surface mesh generator has an option for a merge tolerance distance during the meshing process. Any pair of nodes which are closer together than this merge tolerance can be considered candidates to be automatically merged together. The default

merge tolerance is 0.1 mm. Normally, this merge tolerance serves to eliminate spurious glitches in the CAD modelling. However, in the case of the micro moulding geometries, where the mesh size will be set to a very small value, it is essential that the merge tolerance value is set to a value lower than the target mesh size. A value of 0.01 mm was used in this study and the mesh which resulted for the dog-bone geometry is shown in Figure 11. If this lower mesh merge tolerance was not used, then gross geometry errors occurred in the resulting mesh, as the example shown in Figure 12.

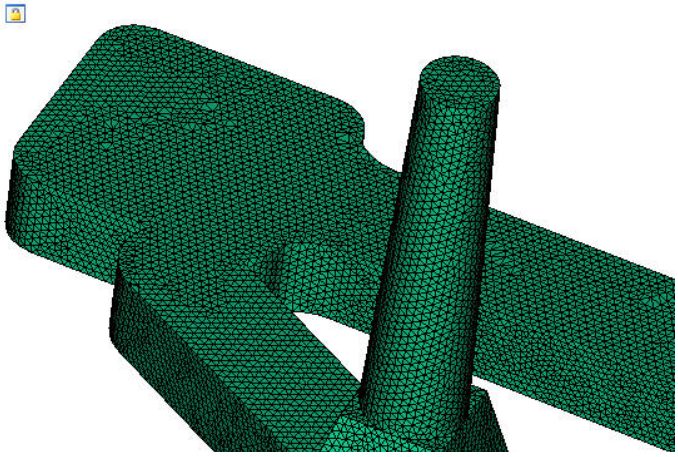

Figure 11 0.1 mm surface mesh created on dog-bone geometry with 0.01 mm merge tolerance

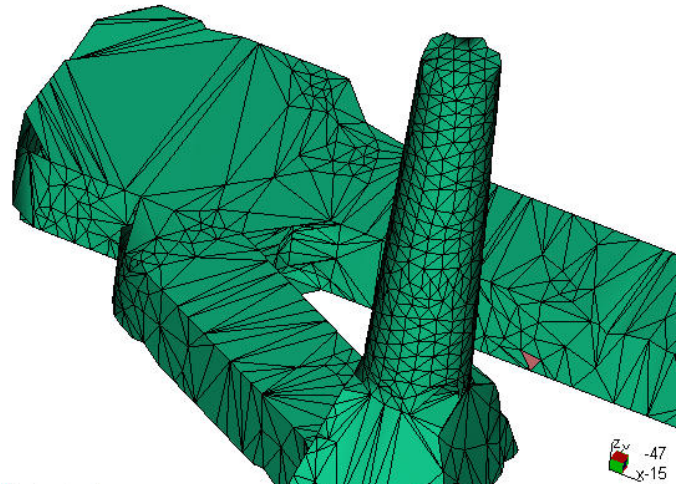

Figure 12 Poor geometry reproduction when default merge tolerance (0.1 mm) was used together with a mesh size of 0.1 mm.

During three-dimensional mesh creation, the Autodesk Moldflow Insight product allows control of a minimum number of layers of tetrahedral elements created through the thickness of all sections of the geometry. This is to ensure a minimum resolution of temperature, shear rate and a viscosity variation is achieved. For the dog-bone geometry, 10 mesh layers of elements were specified as a minimum through the thickness. This corresponded with the cavity thickness of 1 mm and the surface mesh size of 0.1 mm. For the thin flat cavity, a minimum of 6 mesh layers were used due to the shell nature of the geometry. More layers of elements were automatically used in the thicker regions of the geometry.

4. Application of Process Conditions to Simulation

As noted above, numerous inconsistencies exist in the experimental data for both the dog-bone and the thin flat cavity. These inconsistencies create uncertainties about how to best set up the process setting boundary conditions for the micro moulding simulation of these two cases.

4.1 Dog-bone Geometry

In the case of the dog-bone geometry, the full stroke volume is greater than the mould volume to be filled. Compressibility of the polymer melt is insufficient to explain the volume difference, therefore, in the process settings of the simulation setup, the injection stroke was considered to start from a piston position of 21 mm. This meant that the cavity was almost but not yet completely filled when the switch-over to pressure control occurred.

The polymer used in the experiments (BASF H2320 004 POM) was available in the Autodesk Moldflow Insight database of characterised materials, so this material was selected for the analysis. The characterization of this material includes the juncture loss coefficients which model the additional entrance pressure drop due to a contraction (tapered or step change) in the feed system geometry. The mould temperature was set at 50°C and the melt temperature was set as 220°C, matching those used in the moulding experiments.

The injection speed of the piston was recorded by the micro moulding machine through 8 control points in the injection phase. The piston position (stroke) at each of these control points was also recorded. For the simulation, a "ram speed versus ram position" injection profile was used with these recorded values of velocity and position. This input also requires the injection barrel diameter (3 mm) to be input in the machine settings. The advantage of including this injection profile rather than just using a single injection time input is that any profiling of the injection velocity can be included in the analysis, resulting in more accurate pressure predictions. Another advantage of using the piston position data is that the total volume of polymer melt contained in the injection chamber can be included in the compression calculations. As the injection pressure rises and material in the injection chamber is compressed, there will be less volume of material exiting the injection nozzle than the swept volume of the piston movement. The amount of the "lost" volume depends on the volume of material in the injection chamber being compressed, hence the

advantage of using the actual piston positions. This is particularly important for this micro moulding machine due to the design of the metering and injection chambers. The use and position of the metering chamber dictates that all injection should start from the maximum stroke length of 23 mm and then stop at whatever piston position gives the desired shot volume. This is different from conventional injection moulding with a reciprocating screw in which the desired shot volume plus a cushion value is used to determine the screw starting position. In the current experimental study, switchover to pressure control occurred at a piston position of 10.3 mm. This means that the polymer material being compressed ahead of the piston was nearly the same volume again as the shot volume itself, causing the volume "lost" to compression to be proportionally larger than in conventional injection moulding. The compression of polymer in the injection chamber as pressure rises causes the apparent material flow rate to be lower than the set value (typically by between 3% and 10% depending on the injection pressure and amount of material being compressed).

If the injection moulding simulation is performed on the geometry to be filled, as shown in Figure 2, then the injection pressure predicted will be the pressure at the top of the sprue as modelled. However, the injection pressure recorded by the FormicaPlast 1k micro moulding machine is based on the pressure pushing from the injection piston itself. This introduces two potential pressure losses which will not be included in the simulation of the basic geometry:

1. Pressure losses due to the entrance pressure effect (elongational flow) as the polymer enters the narrow nozzle tip from the wider injection chamber (barrel).
2. Friction losses due to the movement of the piston at the injection speed.

An estimate of both of these pressure losses combined could be obtained by performing an air shot with the injection unit moved back from the stationary mould half and purging polymer from the nozzle tip. Such a purge should be done at the same injection speed as used in the actual injection. The injection pressure recorded by the machine during this air shot should be subtracted from total injection pressure recorded during actual moulding to obtain the net pressure required to fill the moulding cavity shown in Figure2.

An estimate of the likely significance of the entrance pressure loss effect can be obtained by performing analyses on the injection geometries which include the nozzle tip contraction. Three such analysis models are shown in Figure 13. One model had a nozzle tip length of 1 mm and diameter of 0.85 mm with a taper from the 3 mm injection chamber diameter over 3 mm. The top of the sprue in the mould has a diameter of 0.85 mm. The second model has a 0.4 mm diameter nozzle tip, with the same length of 1 mm and same taper from the 3 mm injection chamber diameter. The third model has a nozzle tip diameter of 0.4 mm and length of 4 mm with an abrupt diameter change from the 3 mm injection chamber diameter. The authors wish to stress that these nozzle geometries are hypothetical and do

not represent the actually inner geometry of the nozzle used on the FormicaPlast 1k machine. The actual internal nozzle geometry was not known at the time of this study. Only the injection barrel diameter (3 mm) and the average stroke length (16 mm) were based on actual known values. This nozzle tip and injection chamber length were modelled with hot sprue elements (shown in red), meaning that they would be prefilled at the start of analysis and have a hot wall temperature. The average injection chamber length of 16 mm was also included in these models to obtain an estimate of the pressure drop along the length of the injection chamber.

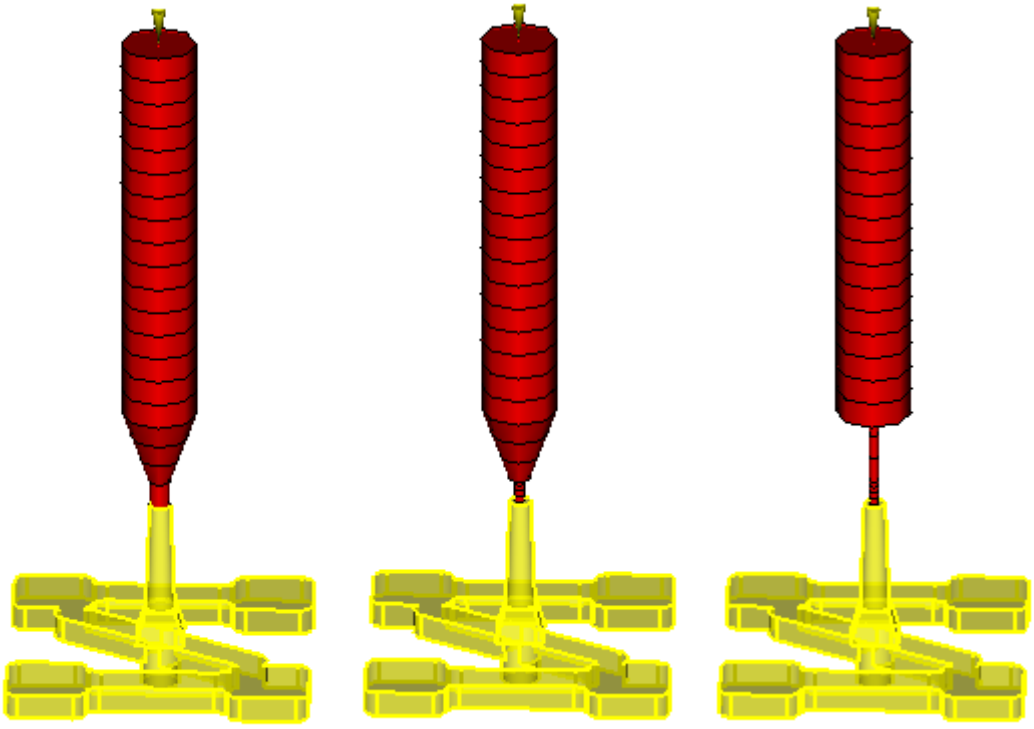

(A) (B) (C)

Figure 13 Hypothetical nozzle tips for dog-bone cavity: (A) 0.85 mm diameter with taper, (B) 0.4 mm diameter with taper, and (C) 0.4 mm diameter with no taper

These three hypothetical nozzle tip geometries will be used in the simulation analyses to illustrate the significance of the nozzle geometry on the injection pressure observed from the injection piston.

4.2 Thin Flat Cavity Geometry

The moulding experiments of the Thin Flat Cavity were performed with a Ineos 100-GA12 PP material. This grade was not available in the Autodesk Moldflow Insight Database of characterised materials, therefore, only an approximately matching polypropylene grade with a similar melt flow index from the same manufacturer could be used, Ineos Acrylics H12Z-00. The mould and melt temperatures of the simulation were set to 60°C and 220°C respectively to match those process settings used during the moulding trials.

For this moulding trial, direct comparison could not be made of the predicted injection pressure with the pressure recorded by the sensor under the ejector pin. This is because the apparent cavity flow rate is so much lower than the set flow rate at the nozzle. It is believed that this is caused by filling or expansion of the disc volume under the injection nozzle, meaning that not all the material injected is reaching the cavity. Since the expansion of the disc volume due to backward movement of the injection nozzle is not modelled in the simulation, the simulation would deliver the full injected volume to the cavity and this would fill the cavities between 3 and 5 times faster than the observed cavity filling times.

For the injection moulding simulation, the apparent average cavity flow rates (see Table 2) were used on a model which contained just the cavity and gate region. Switch-over to pressure control was set to occur only once the cavity reached 100% fill. However, a critical pressure limit is believed to potentially occur earlier than 100% cavity fill as was shown in Figure 7 for the 480 mm/s injection case. Therefore, the comparison of pressure from simulation and moulding will be done at the instant when the pressure stopped rising, or when the cavity was first filled (which-ever was recorded first). The comparison is between the pressures at different locations: The measured pressure is from the transducer under the ejector pin at the nozzle location, while the simulation pressure is from the gate entrance. However, this approximation is considered valid because the injection pressure was not observed to rise until the flow front reached the gate, indicating that the pressure drop along the runner was very small.

The default heat transfer coefficient (HTC) during the filling phase for conventional injection moulding simulation is 5000 W/m^2C. The present geometry is thin enough (0.25mm) to be considered significantly below the cavity thicknesses of conventional injection moulding. Therefore, as a comparison, simulations were also run using a HTC one order of magnitude higher than the default value to test the sensitivity of this high speed filling process to the HTC value.

5. Simulation Results

All simulations were performed using Autodesk Moldflow Insight 2010-R2.

5.1 Dog-bone Shaped Tensile Bar Cavities

Figure 14 shows the predicted injection pressure for four versions of the dog-bone shaped tensile mouldings: The geometry without the injection nozzle modelled ("Cavity Only") plus the three geometries described in Figure 13. These results illustrate the potential significance of the nozzle tip geometry on the pressure recorded to drive the injection piston and therefore the importance of including the actual nozzle tip geometry in the simulation if the accurate pressure comparisons are to be made.

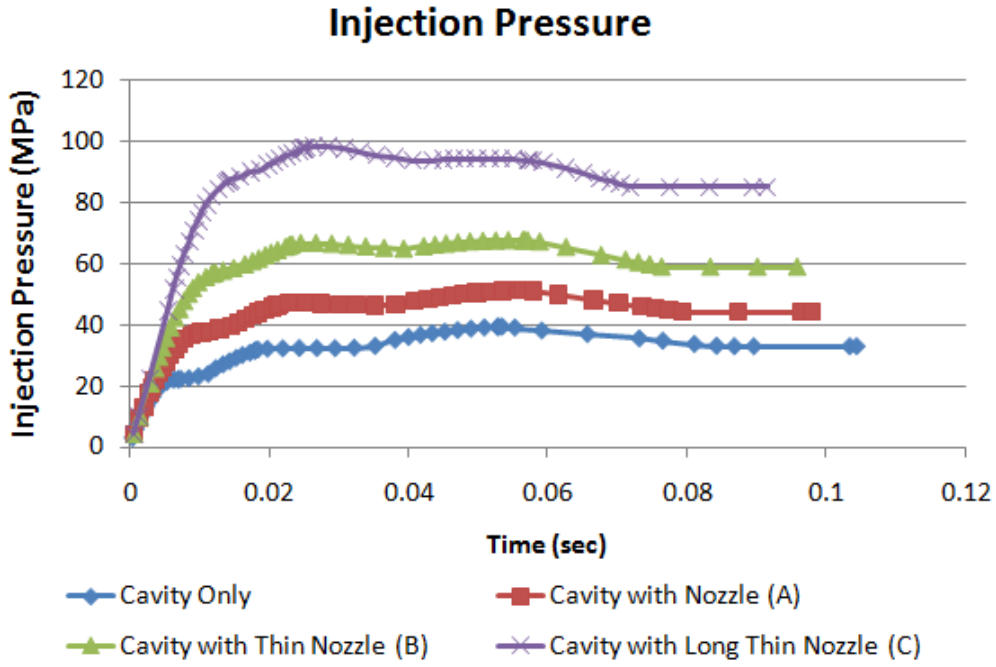

Figure 14 Predicted injection pressure from four variations of dog-bone moulding with different injection nozzles

The main effect of introducing the nozzle and injection chamber geometry is the pressure drop through the narrow nozzle tip and in the contraction.

As shown in the predicted pressure result in Figure 15 for Nozzle (A), the pressure drop along the length of the injection chamber was only 5 MPa. It would be acceptable to not have included this average length of injection chamber in the simulation model. The predicted pressure drop along the contraction and nozzle tip was 11 MPa for this Nozzle (A), 28 MPa for Nozzle (B) and 57 MPa for Nozzle (C).

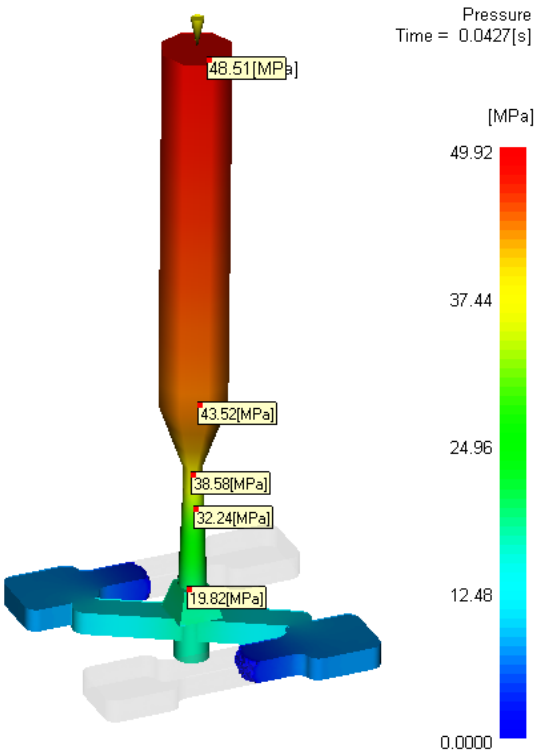

Figure 15 Predicted pressure result during filling with Nozzle (A)

The analyses with Nozzle (A) and Nozzle (B) were also repeated without the juncture loss coefficients to assess the significance of this entrance pressure loss model. The pressure drop through the contraction and nozzle tip was 10 MPa for Nozzle (A) and 20 MPa for Nozzle (B). That is, they were only 1.5 MPa and 8 MPa less than the respective analyses with the juncture loss coefficients, indicating that the effect of the entrance pressure

loss will be only significant when a very narrow nozzle tip is used in this moulding case.

5.2 Thin Flat Cavity Geometry

Figure 16 shows the comparison of measured injection pressure and predicted pressure at the gate for the four apparent cavity flow rates with both the default HTC and higher HTC boundary conditions. In the case of the lowest flow rate, the measured and predicted pressures are shown up to the end of cavity filling. For the other flow rates, the pressure is only shown up to the point in filling when the measured pressure reaches the critical pressure limit. After that point, comparison is not considered to be valid.

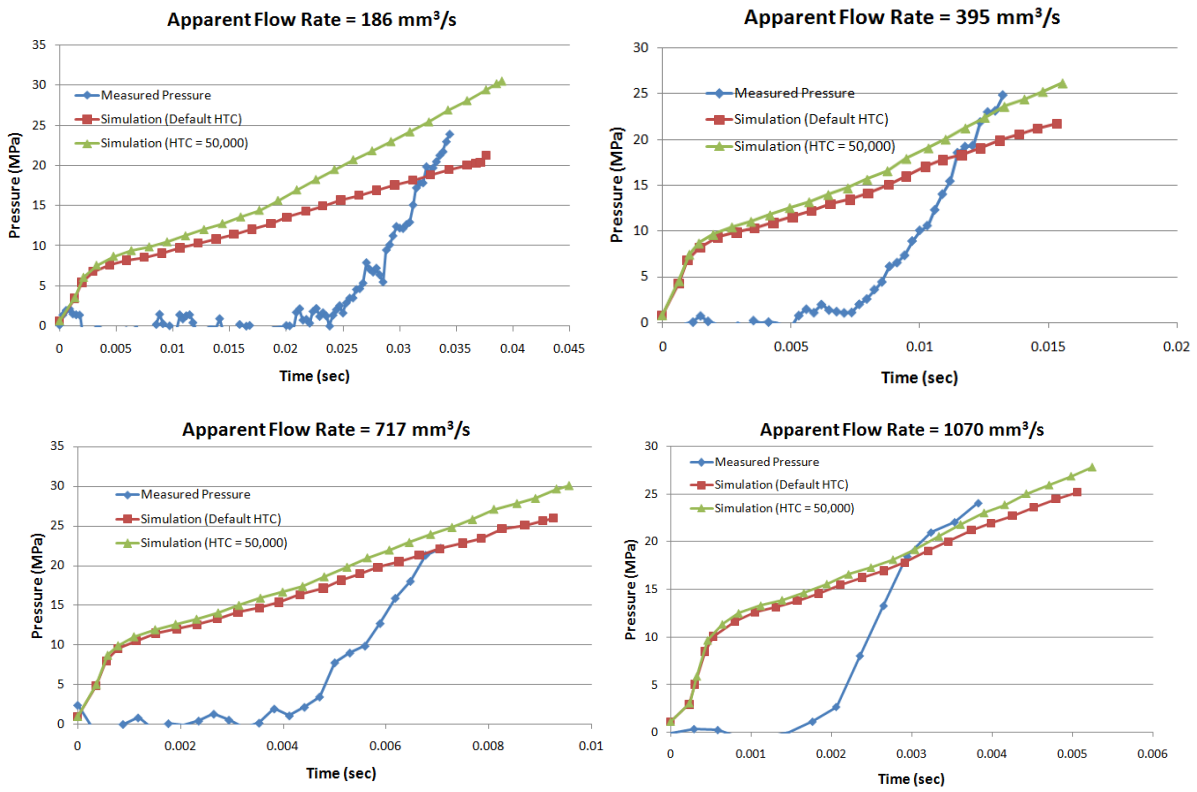

Figure 16 Comparison of measured and predicted pressure for thin flat cavity

Even though the simulations have been run with the observed cavity flow rates, rather than flow rates determined from process monitoring, there is still a large disagreement in the shape of the pressure rise. The timing discrepancy is due to the compressibility of the polymer melt being considered in the simulation. In simulation, the flow rate setting is used to determine a piston velocity and then compression of polymer in the injection barrel and mould mean that the apparent flow rate at the flow front is slower. However, of greater concern is still the lack of agreement in timing of the initial pressure rise. As discussed previously, this may be caused by data filtering or timing problems in the data acquisition.

Using a HTC value one order higher than the default for conventional injection moulding only introduces a small difference in predicted pressure at the higher flow rates and a moderate difference for the slowest flow rate. From this observation, it is not expected that variation of HTC alone can improve agreement between measurement and simulation for micro-injection moulding.

6. Conclusions

A validation study was conducted on two different micro polymer parts (a dog-bone shaped tensile bar and a thin flat cavity geometry), both moulded using micro injection moulding machines (a FormicaPlast 1k by DESMAtec and a Microsystem 50 by Battenfeld respectively) to highlight best practice strategies when performing validation studies of micro moulding simulations. Advantages and issues of flow front analysis

methods such as micro short shots and flow visualization have been presented. The importance of in-process pressure and speed measurements as well as accurate meshing of the micro geometry has been highlighted. Issues in the micro moulding execution (regarding both the process and the machine own geometry) have been underlined in connection with the application of process conditions to simulation. Finally, examples of how the different implementation strategies actually influence the simulation results and the validation study were given.

In conclusion, as far as experimental studies of micro moulding are to be used to validate simulation methodologies, the following aspects must be carefully considered along with consequent recommendations regarding validation studies for micro moulding.

- Parameters used in the finite element mesh preparation, including mesh merge tolerance, must be adjusted from default values for micro moulding studies where characteristic dimensions are much smaller than for conventional injection moulding cases.
- Visualisation of flow front position alone is not sufficiently sensitive to discern accuracy or otherwise of the processing simulation. Use of measured injection pressures or cavity pressures is recommended. However, where available, visualisation of flow front position can assist to confirm (or indicate problems in) the timing of pressure and piston velocity data acquisition.
- Micro moulded short shots, even when produced using a relatively high resolution piston-driven injection unit suitable for micro

moulding, show limitations in terms of accuracy and process/product repeatability, especially when high injection speeds typically employed in micro moulding are employed. Therefore the short shots method, widely used to validate simulations of the injection moulding process at macro scale, is of limited validity when downscaling part dimensions to the sub-millimetre dimensional range.

- Nozzle tip and contraction geometry should be included in the simulation model when the pressure required in order to move the injection piston is to be compared to predicted injection pressure from simulation.
- Juncture loss model coefficient should be included in the rheology data if nozzle contractions are modelled.
- Backflow into the metering piston can cause shot volume to be less than the swept stroke volume. Adjustment must be made for this in the injection velocity control inputs to simulation.
- High sampling rates and high speed data acquisition at high frequencies during processing are required for complete interpretation of the process behaviour.

Acknowledgements

This paper reports work undertaken in the context of the project "COTECH - Converging technologies for micro systems manufacturing". COTECH is a Large Scale Collaborative Project supported by the European Commission in the 7th Framework Programme (CP-IP 214491-2).

References

1. D. Delaunay, P. LE Bot, "Nature of Contact Between Polymer and Mold in Injection Molding. Part I: Influence of a Non-perfect Thermal Contact", *Polymer Engineering & Science*., **40**, 1682 (2000)
2. O. Kemann, L. Weber, C. Jeggy, O. Magotte and F. Dupret, Simulation of the micro injection moulding process, SPE-ANTEC Tech. Papers, (2000).
3. L. Yu, Experimental and numerical analysis of injection moulding with microfeatures, Ph.D. Thesis, Ohio University (2004).
4. A. Gava, G. Tosello, H.N. Hansen, M. Salvador, G. Lucchetta, Proceedings of the 9th International Conference on Numerical Methods in Industrial Forming Processes (NUMIFORM), 307–312 (2007).
5. Chien R.D., Jong W.R., Chen S.C. (2005) Study on the rheological behaviour of polymer melt flowing through micro-channels considering the wall-slip effect, Journal of Micromechanics and Microengineering, Vol.15, Issue 8, pp.1389-1396.
6. W. Cao, O. Hassager and Y. Wang, Polymer Processing Society (PPS) 24th Annual Meeting Proceedings, S08, 141 (2008).
7. P. Kennedy, *Flow Analysis of Injection Molds*. Hanser (1995)

8. C.A. Hieber and S.F. Shen, A Finite Element/Finite Different Simulation of the Injection-Molding Filling Process, J. Non-Newtonian Fluid Mech. 7, 1-32 (1980).
9. DESMAtec, FormicaPlast 1k, http://www.desma-tec.de/en/index.html, October 2009.
10. E.C. Brown, B.R. Whiteside, R Spares, P.D. Coates. Ultrasonic Monitoring of Micromoulding, SPE Antec 2009, pg 2564-2569